Available online at www.sciencedirect.com
ScienceDirect
Ceramics International 37 (2011) 3037–3043
CERAMICS INTERNATIONAL
www.elsevier.com/locate/ceramint

Silver doped lanthanum chromites by microwave combustion method

A.A. Athawale [*,a,b], P.A. Desai [a]

[a] Department of Chemistry, University of Pune, Pune 411007, India
[b] Centre for Nanoscience and Quantum Systems, Pune 411007, India

Received 28 February 2011; received in revised form 20 April 2011; accepted 5 May 2011
Available online 12 May 2011

Abstract

Considering the advantages of microwave combustion technique with the possibility of utilizing cheap precursors, short reaction time and nanocrystalline products, the present work reports the synthesis of silver doped lanthanum chromites. Structural and physicochemical properties were investigated with the help of various characterization techniques. The FTIR spectrum reveals the characteristic metal oxygen bands for Cr–O stretching at 604 cm^{-1}, O–Cr–O bending mode at 419 cm^{-1} and Ag–O bands at 561 cm^{-1} and 443 cm^{-1}. The powder X-ray diffraction patterns exhibit the formation of hexagonal structure with the dopant peaks at 2θ values of 38.3°, 44.1° and 64.4° apart from the peaks corresponding to lanthanum chromite. TGA analysis of the samples shows stable behavior of the product. Nanosized particles with size as small as ~7–8 nm and larger ones ~20–26 nm are observed from transmission electron micrographs. Room temperature magnetic study exhibits hysteresis loop formation during magnetization of samples.

Keywords: Lanthanum chromites; Silver doping; Microwave synthesis; FTIR analysis; X-ray diffraction analysis; Magnetic properties

1. Introduction

Lanthanum based perovskites (ABO_3) find interesting applications such as thermal indicators and barriers [1,2], interconnect materials for SOFCs [3], ionic conductors [4] and photoctalysts [5], due to their high temperature and chemical stability. The structural characteristics of these materials can be modified when synthesized in nanosize together with good compositional homogeneity and stoichiometry [6–13]. They constitute a good class of combustion catalysts as they are found to be relatively stable in both oxidizing and reducing atmospheres [14]; however, sometimes they are less efficient. Attempts to enhance their efficiency include doping these perovskites with noble metals, such as Rh, Ag and Au [15–20]. Both A site and B site doping are possible bearing mixed valence states and enhanced mobility of oxygen in the lattice [21,22].

The method of synthesis adopted also influences the material properties significantly. Most popular methods of synthesis include hydrothermal, spray pyrolysis, solid state reaction, microwave aided synthesis, sol–gel [23–39], etc.

In the present work, we report the synthesis of nanoparticles of silver doped lanthanum chromite for the first time. The samples were synthesized by microwave combustion method; partial doping at both A site and B site have been achieved with short reaction time of few minutes yielding perovskites of the types $La_{1-x}Ag_xCrO_3$ and $LaCr_{1-x}Ag_xO_3$. Further, the influence of dopant concentration, fuel/oxidizer ratio and precursor salts on material properties is investigated. Thus, the main purpose of this study is to explore the structural and ionic changes in the substituted perovskite with reference to pristine sample.

2. Experimental details

All the chemicals used were of A.R. grade. The salt precursors, i.e. lanthanum nitrate ($La(NO_3)_3{\cdot}6H_2O$), chromium nitrate ($Cr(NO_3){\cdot}9H_2O$) and urea (NH_2CONH_2) as fuel were from Loba Chemie, India, while silver nitrate ($AgNO_3$) was from Qualigens, India. Lanthanum chromite was synthesized by initially mixing the precursor salts together in stoichiometric amounts, i.e. 1:1 equimolar ratio followed by the addition of urea as fuel (0.4 M), and to this was added ~50 ml of double distilled water. The stoichiometric composition of the mixture

* Corresponding author at: Department of Chemistry, University of Pune, Pune 411007, India. Tel.: +91 020 25601395/566/561; fax: +91 020 25691728.
E-mail address: agbed@chem.unipune.ac.in (A.A. Athawale).

0272-8842/$36.00
doi:10.1016/j.ceramint.2011.05.008

was calculated based on the oxidizing valencies of metal nitrates and reducing valency of urea [40]. Silver doped samples were prepared by partial substitution of host atoms (La or Cr) by varying the concentration of added silver from 0.02 to 0.06 M, the molar concentrations of host atoms in the reaction were also varied proportionately. The resulting mixtures (for undoped and doped perovskites) were stirred for few minutes at room temperature and subjected to evaporation on a hot plate so as to obtain a gel. The gels were subjected to microwaves (0.1–0.9 kW power) using a domestic microwave oven (MG-555F Model) for auto combustion and the resulting products were cooled to room temperature. During synthesis, the fuel to oxidizer ratio was maintained as 1 while, the irradiation time was varied from 5 to 10 min so as to obtain pure phase products. The powders were characterized using various analytical techniques.

3. Characterization

Fourier transform infrared spectra (FTIR) of all the samples were recorded on a Shimadzu 8400 spectrophotometer over the range of 400–4000 cm^{-1} using KBr as a mulling agent. X-ray diffraction analysis of the powders was carried out on a Bruker AXSD-8 Advance X-ray diffractometer with monochromatic CuKα radiation (λ = 1.5406 Å). Silicon was used as an external standard for correction due to instrumental broadening. Diffraction data were collected from 20° to 80° at a scan rate of 0.1°/min. Energy dispersive analysis of X-rays (EDAX) was taken on an analytical instrument (JEOL JSM 6360A). The data were recorded by coating the films of the samples with Ag–Pd alloy using vapor deposition technique. Transmission electron micrographs (TEMs) of the samples were observed under the Philips CM-200 instrument at an accelerating voltage of 200 kV. Suspensions of the samples in isopropanol were well dispersed and loaded on carbon coated grids of 200 mesh size. The grids were then dried under IR lamp and viewed under the microscope. The TG–DTA curves of samples were recorded in an inert atmosphere at a heating rate of 10 °C min^{-1} using a Shimadzu instrument (Model DTG-60H). Lakeshore's Vibrating Sample Magnetometer (Model 7307) was used to perform magnetic measurements.

4. Results and discussion

The products were obtained through an exothermic reaction occurring between the reactant precursor's (metal nitrates) and urea as a fuel.

The combustion reaction can be represented as follows:

$$\text{Precursor A} + \text{Precursor B} + \text{Dopant} + \text{Fuel} \xrightarrow[\text{Microwave combustion}]{\Delta} \left.\begin{array}{l} A_{1-x}D_xBO_3 + H_2O\uparrow + N_2\uparrow + CO_2\uparrow \\ \text{or} \\ AB_{1-X}D_XO_3 + H_2O\uparrow + N_2\uparrow + CO_2\uparrow \end{array}\right\} \quad (1)$$

Precursor A ($La(NO_3)_3.6H_2O$), Precursor B ($Cr(NO_3).9H_2O$), Dopant ($AgNO_3$) and Fuel (NH_2CONH_2)

During synthesis, the nitrates readily melt in their water of crystallization and aqueous solutions always absorb microwave radiations efficiently which are the source of energy. Additional heat is evolved upon oxidation of chromium which takes place during decomposition of nitrate salts. The evolved heat is the cause for continuous heating of sample after removal of water leading to decomposition of the precursors to give oxide phase.

The powder samples of $LaCrO_3$, $La_{1-x}Ag_xCrO_3$ $LaCr_{1-x}Ag_xO_3$ (x refers to the fraction of La and Cr substituted by Ag) thus obtained were analysed using various analytical techniques. From the results, it was observed that the microwave power, oxidizer to fuel ratio and irradiation time determined the purity of the samples. At microwave power below 0.42 kW the product formation is not observed, at 0.42 kW partial product formation takes place while, 0.56 kW power yields pure phase product. At higher power levels the reaction is observed to be explosive in nature. The optimum irradiation time to obtain pure phase product is observed to be 10 min with an oxidizer to fuel ratio of 1.

‘4.1. FT-IR spectroscopy

Preliminary analysis of samples to ensure the formation of products was carried out by recording the FTIR spectrum of each of the products. Fig. 1(a) and (b) shows the FTIR spectra of as obtained samples and the one sintered at 800 °C for 4 h, respectively. The absorption peaks at 600 and 400 cm^{-1} can be ascribed to Cr–O bond and O–Cr–O deformation vibrations indicating formation of product, while, narrow bands at 1085–1385 cm^{-1} correspond to NO_3^- of unreacted precursor salts and N–H stretching is observed at 1485 cm^{-1}.

In Fig. 1(c) and (d) are given the FTIR spectra of silver doped (both A site and B site), lanthanum chromite samples which exhibit increment in band assignment of Cr–O stretching and O–Cr–O deformation vibrations implying substitution of Ag^+ ions at lanthanum and chromium sub lattice. The bands at 561 $cm^{-1}$and 443 cm^{-1} represent Ag–O bond formation.

The close frequency correlation of these bands in the spectra with those reported in the literature [41–43] confirms the presence of perovskite like oxide together with doping of silver (Ag^+) ions in A and B sub lattice.

4.2. X-ray diffraction analysis

Fig. 2 shows the X-ray diffractograms of the $LaCrO_3$ samples synthesized at 0.42 kW and 0.56 kW microwave power and the latter sample sintered at 200 and 800 °C for a period of 4 h. Comparison of the X-ray diffractograms reveals the formation of pure phase product at microwave power of

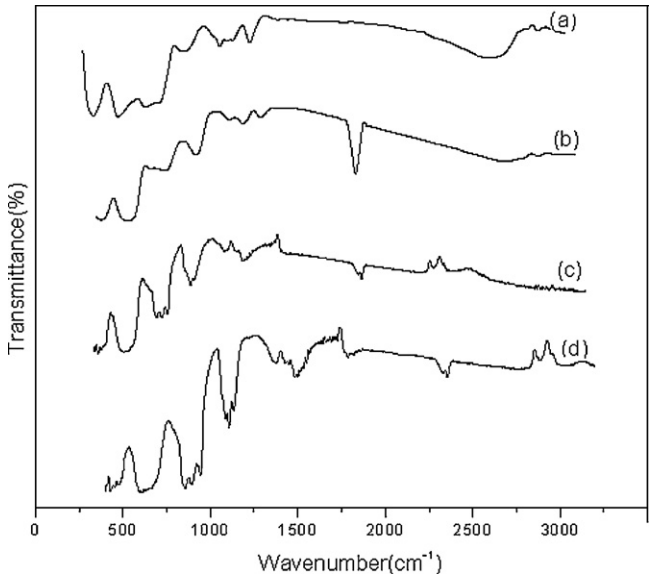

Fig. 1. FT-IR spectra of samples (a) as synthesized $LaCrO_3$, (b) sintered at 800 °C, (c) $La_{0.06}Ag_{0.02}CrO_3$ and (d) $LaCr_{0.06}Ag_{0.02}O_3$.

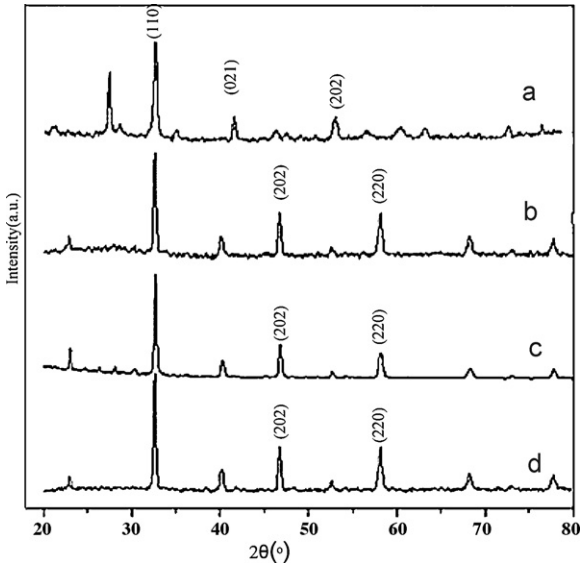

Fig. 2. X-ray diffractograms of lanthanum chromite samples synthesized at (a) 0.42 kW and (b) 0.56 kW microwave power (c) sample sintered at 200 °C and (d) 800 °C.

0.56 kW whereas at 0.42 kW power presence of unreacted precursor salts can be noted, the crystallinity of the product is enhanced on sintering the sample. The peaks at 2θ values of 32.3, 39.9, 46.4, 67.8 and 77.1 represent characteristic planes (1 1 0), (0 2 1), (2 0 2), (2 2 0) and (3 1 2) of hexagonal $LaCrO_3$ (PDF No. 33-0702) while reactant peak is observed at 27.9, respectively (PDF No. 22-1126). The structure factor (intensity of reflection) is dependent on both, the positions of each atom and electron density distribution during phase formation.

X-ray diffractograms of Ag doped (both A site and B site) $LaCrO_3$ are shown in Figs. 3 and 4. The dopant concentration was varied from 0.02 to 0.06 M. Peaks corresponding to metallic silver are observed at 2θ values of 38.3, 44.1 and 64.4

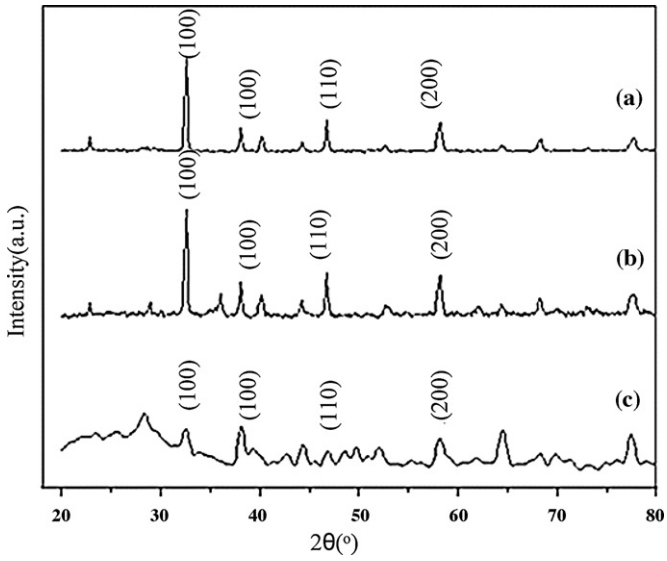

Fig. 3. X-ray diffractograms of samples with silver doped at A site (a) 0.02 M, (b) 0.04 M and (c) 0.06 M.

in addition to the characteristic peaks of lanthanum chromite. The data have been correlated with JCPDS pattern (04-783). Further, increment in the intensity of the peak corresponding to silver is observed with the increase in dopant concentration. Peak at 27.9 at higher doping level (0.06 M of Ag) depicts the presence of unreacted precursor salts.

The crystallite size of the particles calculated using the Scherrer formula [44,45], by considering the half widths of the XRD peaks is given in Table 1, and dopant concentration is expressed as a fraction of host atoms. The lattice parameters exhibit significant differences on Ag doping in comparison to $LaCrO_3$. The expansion in volume can be attributed to the mismatch of ionic radii and co-ordination number (i.e. dodecahedron and polyhedron). The table also includes the theoretical densities calculated for each lattice. The differences

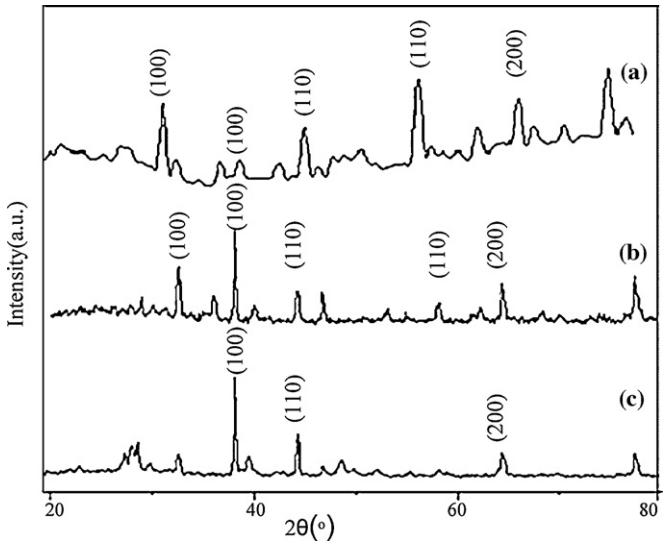

Fig. 4. X-ray diffractograms of samples with silver doped at B site (a) 0.02 M, (b) 0.04 M and (c) 0.06 M.

Table 1
Calculated lattice parameters of (a) $LaCrO_3$, (b) $La_{0.06}Ag_{0.02}CrO_3$, (c) $La_{0.02}Ag_{0.06}CrO_3$, (d) $LaCr_{0.06}Ag_{0.02}O_3$ and (e) $LaCr_{0.02}Ag_{0.06}O_3$.

Sr. No.	Sample	*d*-spacing	V Cell $a^3(m^3)$ ($x10^{-29}$)	Theoretical density g/cm^3	Crystallite Size (nm)	Direct (nm)
(a)	$LaCrO_3$	2.730	4.97	1.915	~57	~57
(b)	$La_{0.06}Ag_{0.02}CrO_3$	2.326	16.27	1.915	~28	~7
(c)	$La_{0.02}Ag_{0.06}CrO_3$	2.326	16.27	1.879	~23	~8
(d)	$LaCr_{0.06}Ag_{0.02}O_3$	2.352	16.27	1.968	~34	~26
(e)	$LaCr_{0.02}Ag_{0.06}O_3$	2.352	16.27	2.03	~35	~20

Table 2
EDAX data of $LaCrO_3$, silver doped at A site (0.02 M and 0.06 M) and silver doped at B site (0.02 M and 0.06 M).

Sample	Elemental composition (at.%)			
	La	Cr	O	Ag
$LaCrO_3$	7.89	8.64	83.47	–
$La_{0.06}Ag_{0.02}CrO_3$	2.57	5.24	89.34	2.85
$La_{0.02}Ag_{0.06}CrO_3$	0.49	0.33	99.07	0.11
$LaCr_{0.06}Ag_{0.02}O_3$	1.79	1.79	95.70	0.71
$LaCr_{0.02}Ag_{0.06}O_3$	21.05	8.16	65.16	5.63

in the theoretical densities can be accounted in terms of variation in the unit cell volume, molar mass of compounds and the A or B site deficiencies in the crystal lattice. The results of EDAX are summarized in Table 2, in case of lanthanum chromite the atomic ratio for La/Cr is expected to be 1, however, in the present case lower ratio indicates the formation of Cr-rich phase. Partial substitution of dopant at A site with higher molar concentration (0.06 M) of silver exhibits a shift in composition to oxygen excess in perovskite with a slight B site ion deficiency.

EDAX of samples with B site doping (Table 2) clearly shows the formation of silver rich phase of the perovskite at lower doping level (0.02 M) while at higher concentration of silver (i.e. 0.06 M) oxygen ion deficiency can be observed. Thus, the solid phase concentrations of elements in the sample could be determined, the discrepancy in the quantitative data is attributable to volatilization of chromium vapor [5] during microwave combustion synthesis.

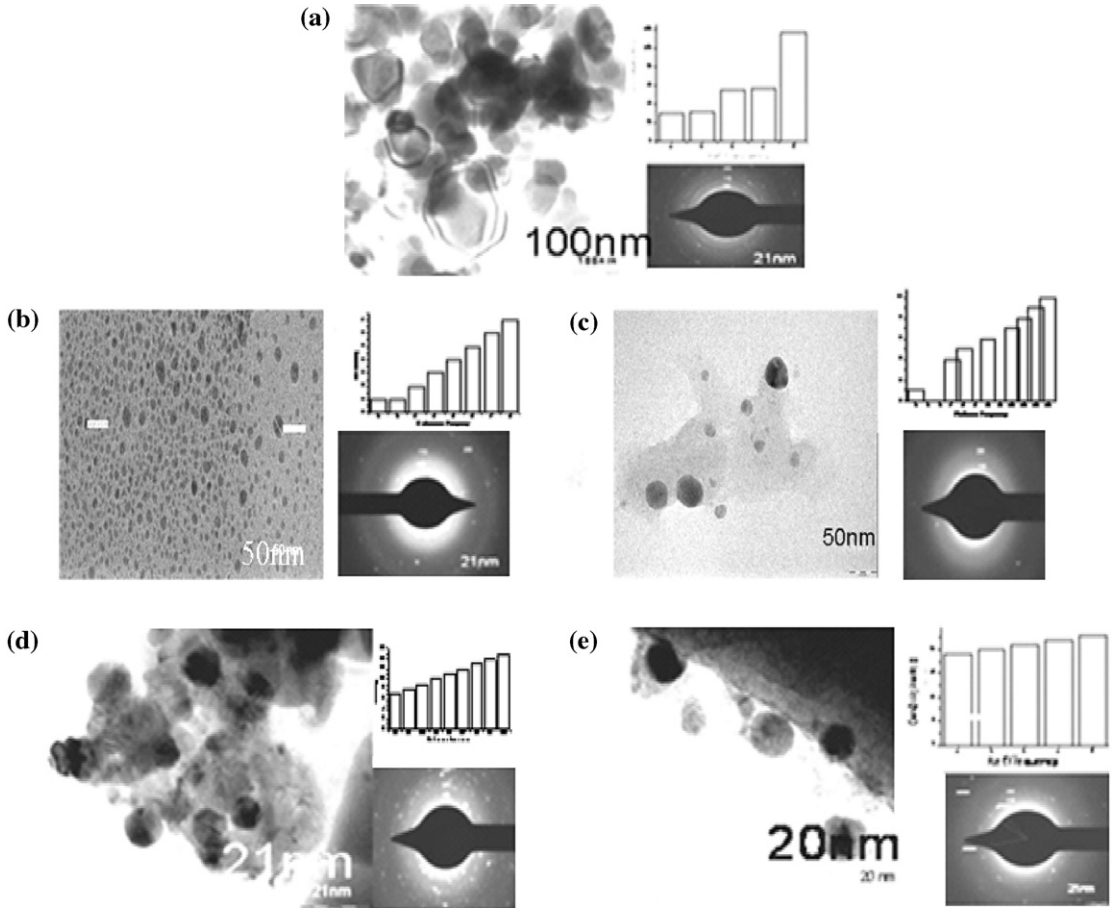

Fig. 5. Transmission electron micrographs, bar diagram as inset and SAED patterns for (a) $LaCrO_3$, (b and c) A site doped $La_{1-x}Ag_xCrO_3$ (x = 0.02 and 0.06) and (d and e) B site doped $LaCr_{1-x}Ag_xO_3$ (x = 0.02 and 0.06).

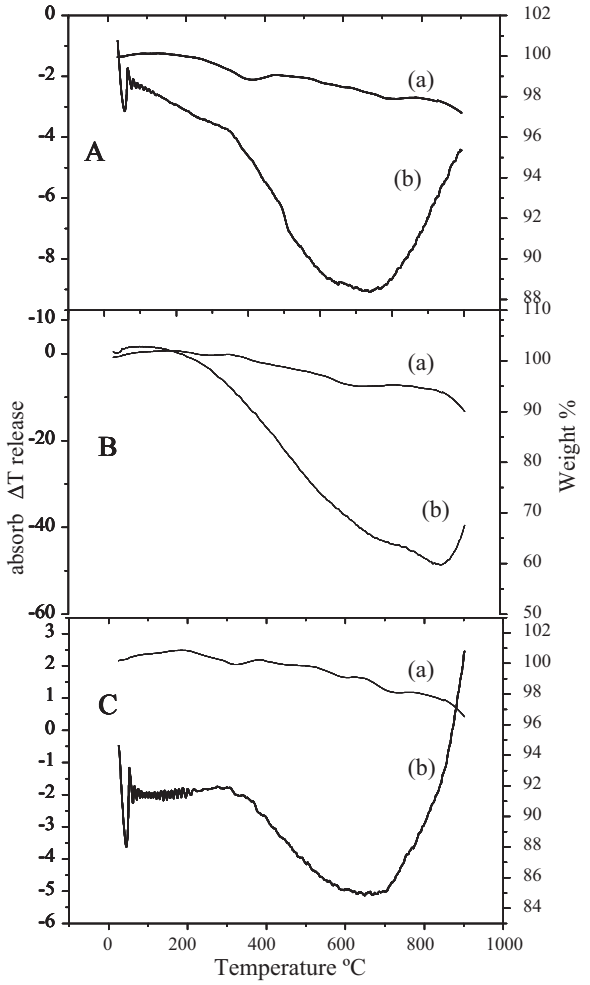

Fig. 6. TG (a) and DTA (b) plots of (A) $LaCrO_3$, (B) $La_{0.06}Ag_{0.02}CrO_3$ and (C) $LaCr_{0.06}Ag_{0.02}O_3$.

4.3. Morphological evidence

The micrograph (TEM) of lanthanum chromite powder synthesized by microwave combustion route is shown in Fig. 5(a). From the micrograph, one can note the formation of particles with mixed morphologies, some being spherical while others appear to be hexagonal in shape. Individual particles with clear grain boundaries are observable. The particles are relatively large in size with average particle size of ∼57 nm. The size distribution appears to be broad ∼30–118 nm shown by the bar diagram with majority being on the higher side. Ring pattern exhibits polycrystalline nature of the sample Fig. 5(a).

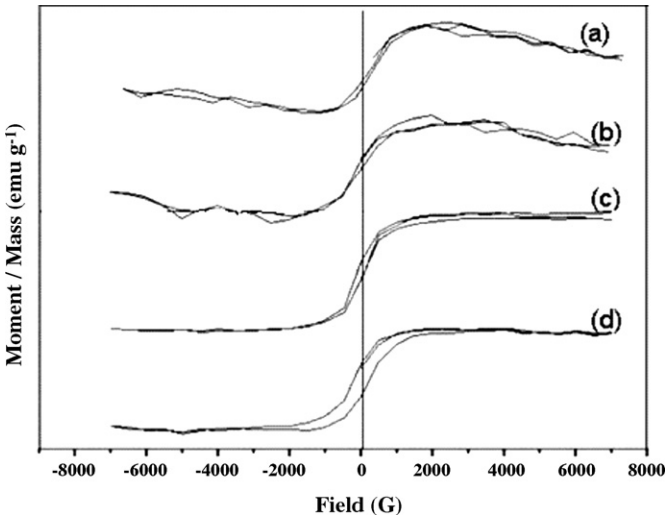

Fig. 7. Magnetograms of (a) as synthesized $LaCrO_3$, (b) $LaCrO_3$ sintered at 800 °C, (c) silver doped at A site (0.02 M) and (d) silver doped at B site (0.02 M).

Micrographs of samples with silver doped at A site (0.02 M and 0.06 M) are shown in Fig. 5(b) and (c), respectively. The particles in both the samples show spherical morphology, the size being significantly smaller in comparison to that of pure lanthanum chromite. The average size of particles is ∼7–8 nm in both the cases. The relative density of smaller particles is higher at 0.02 M doping level Fig. 5(b). Higher silver concentration of 0.06 M Fig. 5(c) leads to a slight increase in particle size distribution of ∼4–15 nm. Diffraction patterns exhibit array of spots related to de Broglie wavelength and polycrystallinity of the samples.

Fig. 5(d) and (e) depicts the micrographs of lanthanum chromite with silver doped at B site. Irregular shaped morphology of the particles can be observed from the micrographs. The particle size distribution is ∼22–30 nm and ∼18–22 nm, respectively for 0.02 and 0.06 M doped silver (Table 1). Polycrystalline nature of the samples is observed from the diffraction pattern.

The decrease in particle size in case of doped samples can be accounted in terms of distortion in structure brought about by the dopant ions.

4.4. Thermal analysis

The thermograms (curves *a*) for $LaCrO_3$, $La_{0.06}Ag_{0.02}CrO_3$ and $LaCr_{0.06}Ag_{0.02}O_3$ are shown in Fig. 6. A negligible weight loss of 1–2% is noted which can be attributed to trace levels of

Table 3
Magnetic data of (a) $LaCrO_3$, (b) sample sintered at 800 °C and (c) $La_{0.06}Ag_{0.02}CrO_3$ and $LaCr_{0.06}Ag_{0.02}O_3$.

Sample name	Saturation magnetization (Ms) (E−3 emu g^{-1})	Retentivity (Mr) (E−3 emu g^{-1})	Coercivity (HCi) (G – Gauss)
$LaCrO_3$	21.679	1.1191	45.844
$LaCrO_3$ sintered at 800 °C 4 h	32.189	2.2752	88.27
$La_{0.06}Ag_{0.02}CrO_3$	79.516	12.568	74.70
$LaCr_{0.06}Ag_{0.02}O_3$	62.265	19.018	231.88

volatiles including adsorbed water, etc. Differential thermograms (curves *b*) exhibit an endotherm at 90 °C corresponding to desorption of adsorbed water. The endotherm at temperature ~600 °C is attributable to the decomposition of traces of precursors and organic fuel (urea).

4.5. Magnetic properties

Fig. 7 shows the magnetograms obtained for $LaCrO_3$ and doped samples. Hysteresis loops are observed in each case with low coercivity indicating formation of soft chromites. Table 3 gives the values of saturation magnetization (Ms), retentivity (Mr) and coercivity (HCi) evaluated from the figure. The doped samples exhibit increase in saturation magnetization that can be attributed to non magnetic nature of Ag.

5. Conclusions

$LaCrO_3$ and silver doped lanthanum chromite nanoparticles have been synthesized by microwave combustion route. Pure phase products are obtained at microwave power of 0.56 kW, irradiation time of 10 min and fuel to oxidizer ratio of 1. Average size of $LaCrO_3$ particles is ~57 nm, while the silver doped samples have a finer particle size of ~7–8 and 20–26, respectively, for A site and B site doping. Increase in coercivity and saturation magnetization values of doped samples is attributed to non magnetic nature of silver.

Acknowledgements

The funding for this work has been provided by DST of India and DST Unit on Nanoscience, PAD acknowledges DST for JRF. The authors gratefully acknowledge CNQS, Department of Physics, University of Pune for XRD analysis, SAIF, IIT Powai, Mumbai for TEM analysis.

References

[1] Yu.L. Suponitskii, Thermal properties and thermo chemistry of lanthanide chromates, Russ. Chem. Bull. Int. Ed. 54 (2) (2005) 294–299.
[2] W.-Y. Ho, C.-H. Hsu, M.-H. Tsai, Y.-S. Yang, D.-Y. Yang, Interlayer effect on characterization of the La–Cr–O coatings with post sputtering annealing treatment, Appl. Surf. Sci. 256 (2010) 2705–2710.
[3] S.A. Suvorov, A.P. Shevchik, Chemical equilibria involving lanthanum chromite, Refract. Ind. Ceram. 45 (2) (2004) 94–99.
[4] T. Akashi, Y. Maruyama, T. Goto, Transport of lanthanum ion and hole in $LaCrO_3$ determined by electrical conductivity measurements, Solid State Ionics 164 (2003) 177–183.
[5] J. Jose, J. Ameta, P.B. Punjabi, V.K. Sharma, C. Suresh, Lanthnaum chromite oxide catalyst: synthesis, characterization and photocatalytic activity shown in Azure-B Ameta, Bull. Catal. Soc. India 6 (2007) 110–118.
[6] N.E. Cipollini, B.L. Wu, S. Haig, J. Yamanis, Beneficiated lanthanum chromite for low temperature firing, US Patent 643,255 (1992).
[7] Z. Zhong, Lanthanum chromite based ceramic interconnects with low sintering temperature, Solid State Ionics 177 (2006) 757–764.
[8] C. Chettapongsaphan, S. Charojrochkul, S. Assabumrungrat, N. Laosiripojana, Preparation of high surface area $LaCrO_3$ for later application in solid oxide fuel cell (SOFC), Asian J. Energy Environ. 9 (1/2) (2008) 101–119.
[9] J.G.M. Furtado, R.N. Oliveira, Development of lanthanum chromites-based materials for solid oxide fuel cell interconnects, Rev. Mater. 13 (1) (2008) 147–153.
[10] P. Vernoux, Lanthanum chromite as an anode material for solid oxide fuel cells, Ionics 3 (1997) 270–276.
[11] Z.J. Feng, C.L. Zeng, $LaCrO_3$-based coatings deposited by high-energy micro-arc alloying process on a ferritic stainless steel interconnect material, J. Power Sources 195 (2010) 4242–4246.
[12] G. Stakkestad, J. Sjoblom, B. Grung, T. Sigvartsen, Surface chemistry of lanthanum chromite. I. Multivariate data modeling of Brunauer–Emmett–Teller surface area by the use of particle size distribution data from photon-correlation spectroscopy measurements, Colloid. Polym. Sci. 277 (1999) 627–633.
[13] G. Stakkestad, J. Sjoblom, B. Grung, T. Sigvartsen, Surface chemistry of lanthanum chromite. II. Multivariate data modelling of the isoelectric point by the use of surface composition data achieved from X-ray photoelectron spectroscopy measurements, Colloid. Polym. Sci. 277 (1999) 174–183.
[14] K.P. Ong, P. Blaha, P. Wu, Origin of the light green color and electronic ground state of $LaCrO_3$, Phys. Rev. B 77 (2008) 073102–073104.
[15] N. Russo, D. Fino, G. Saracco, V. Specchia, Promotion effect of Au on perovskite catalysts for the regeneration of diesel particulate filters, J. Catal. 29 (2) (2005) 459–469.
[16] D.-J. Liu, M. Krumpelt, Activity and structure of perovskites as diesel-reforming catalysts for solid oxide fuel cell, Int. J. Appl. Ceram. Technol. 2 (4) (2005) 301–307.
[17] S.W. Sofie, P. Gannon, V. Gorokhovsky, Silver–chromium oxide interactions in SOFC environments, J. Power Sources 191 (2009) 465–472.
[18] I.K. Kamilov, A.G. Gamzatov, A.M. Aliev, A.B. Batdalov, Sh.B. Abdulvagidov, O.V. Melnikov, O.Yu. Gorbenko, A.R. Kaul, Kinetic effects in manganites $La_{1-x}Ag_yMnO_3$ ($y \leq x$), J. Exp. Theor. Phys. 105 (4) (2007) 774–781.
[19] S. Barison, M. Battagliarin, S. Daolio, M. Fabrizio, E. Miorin, P.L. Antonucci, S. Candamano, V. Modafferi, E.M. Bauer, C. Bellitto, G. Righini, Novel $Au/La_{1-x}Sr_xMnO_3$ and $Au/La_{1-x}Sr_xCrO_3$ composites: catalytic activity for propane partial oxidation and reforming, Solid State Ionics 177 (2007) 3473–3484.
[20] N. Russo, D. Fino, G. Saracco, V. Specchia, Promotion effect of Au on perovskite catalysts for the regeneration of diesel particulate filters, Catal. Today 137 (2008) 306–311.
[21] M. Mori, Y. Hiei, N.M. Sammes, Sintering behavior and mechanism of Sr-doped lanthanum chromites with A site excess composition in air, Solid State Ionics 23 (1) (1999) 103–111.
[22] V. Vashook, J. Zosel, W. Preis, W. Sitte, U. Guth, A-deficient chromites–titanates with the perovskite-type structure: synthesis and electrical conductivity, Solid State Ionics 175 (2004) 441–444.
[23] C. Rendón-Angeles, K. Yanagisawa, Z. Matamoros-Veloza, M.I. Pech-Canul, J. Mendez-Nonell, S. Diaz-de la Torre, Hydrothermal synthesis of perovskite strontium doped lanthanum chromite fine powders and its sintering, J. Alloys Compd. 504 (1) (2010) 251–256.
[24] Y. Jiang, J. Gao, M. Liu, Y. Wang, G. Meng, Synthesis of $LaCrO_3$ films using spray pyrolysis technique, Mater. Lett. 61 (2007) 1908–1911.
[25] J. Cheng, A. Navrotsky, Energetics of $La_{1-x}A_xCrO_3$ (A = Ca or Sr), J. Solid State Chem. 178 (2005) 234–244.
[26] M. Iwasaki, H. Takizawa, K. Uheda, T. Endo, M. Shimada, Microwave synthesis of $LaCrO_3$, J. Mater. Chem. 8 (1998) 2765–2768.
[27] Y.S. Malghe, S.R. Dharwadkar, $LaCrO_3$ powder from lanthanum trisoxalatochromate(III) (LTCR) precursor microwave aided synthesis and thermal characterization, J. Therm. Anal. Calorim. 91 (2008) 915.
[28] A.R. Yavari, A. Inoue, D. Morris, R. Schulz, Microwave assisted combustion synthesis of $LaCrO_3$ nanopowders, J. Metastable Nanocryst. Mater. 22 (2004) 91–96.
[29] A.S. Mukasyan, P. Dinka, Novel approaches to solution–combustion synthesis of nanomaterials, Int. J. Self-Propag. High-Temp Synth. 16 (2007) 23–25.
[30] H.K. Park, Y.S. Han, D.K. Kim, C.H. Kim, Synthesis of $LaCrO_3$ powders by microwave induced combustion of metal nitrate–urea mixture solution, J. Mater. Res. Sci. Lett. 17 (1998) 785–787.

[31] S.M. Khetre, H.V. Jadhav, S.R. Bamane, Synthesis and characterization of nanocrystalline $LaCrO_3$ by combustion route, Rasayan J. Chem. 2 (2009) 174–178.
[32] M. Panneerselvam, K.J. Rao, Microwave preparation and sintering of industrially important perovskite oxides: $LaMO_3$ (M = Cr, Co, Ni), J. Mater. Chem. 13 (2003) 596–601.
[33] A.S. Vanetsev, Yu.D. Tretyakov, Microwave assisted synthesis of individual and multicomponent oxides, Russ. Chem. Rev. 76 (5) (2007) 397–413.
[34] W. Tu, H. Liu, Rapid synthesis of nanoscale colloidal metal clusters by microwave irradiation, J. Mater. Chem. 10 (2000) 2207–2211.
[35] Tanu Minami, Preparation of alumina products, Fire Synthesis 5 (2) (2000) 50–57.
[36] K.J. Rao, B. Vaidhyanathan, M. Ganguli, P.A. Ramakrishnan, Synthesis of inorganic solids using microwaves, Chem. Mater. 11 (1999) 882–895.
[37] D.E. Clark, W.H. Suttan, Microwave processing of materials, Annu. Rev. Mater. Sci. 6 (2) (1996) 299–331.
[38] E. Balakrishnan, M.I. Nelson, X.D. Chen, Microwave assisted ignition to achieve combustion synthesis, J. Appl. Math. Decis. Sci. 5 (3) (2001) 151–164.
[39] I.A. Zhigalkina, T.D. Nikolaeva, Yu.L. Suponitskii, B.I. Polyak, Synthesis of lanthanum chromite by sol gel method, Glass Ceram. 55 (5–6) (1998) 182–185.
[40] S.R. Jain, K.C. Adiga, V.R. Paiverneker, A new approach to thermochemical calculations of condensed fuel-oxidizer mixtures, Combust. Flame 40 (1981) 71–79.
[41] G.V. Subha Rao, C.N.R. Rao, J.R. Ferraro, Infrared spectra and electronic spectra of rare earth perovskites: ortho-chromites, manganites and ferrites, Appl. Spectrosc. 24 (1970) 436–444.
[42] G.A. Tompsett, N.M. Sammes, Characterisation of the SOFC material, $LaCrO_3$, using vibrational spectroscopy, J. Power Sources 130 (2004) 1–7.
[43] G.I.N. Waterhouse, G.A. Bowmaker, J.B. Metson, The thermal decomposition of silver(I, III) oxide: a combined XRD, FT-IR and Raman spectroscopic study, Phys. Chem. Chem. Phys. 3 (2001) 3838–3845.
[44] P. Scherrer, Bestimmung der Grösse und der inneren Struktur von Kolloidteilchen mittels Röntgenstrahlen, Nachr. Ges. Wiss. Göttingen 26 (1918) 98–100.
[45] J.I. Langford, A.J.C. Wilson, Scherrer after sixty years: a survey and some new results in the determination of crystallite size, J. Appl. Crystallogr. 11 (1978) 102–113.